Synthesis and *In Vitro* Evaluation of the Anti-Viral Activity of N-[4-(1*H*(2*H*)-benzotriazol-1(2)-yl)phenyl]alkylcarboxamides

Antonio Carta[a,*], Giovanni Loriga[a], Sandra Piras[a], Giuseppe Paglietti[a], Marco Ferrone[b], Maurizio Fermeglia[b] and Sabrina Pricl[b], Paolo La Colla[c,*], Barbara Secci[c], Gabriella Collu[c] and Roberta Loddo[c]

[a]*Dipartimento Farmaco Chimico Tossicologico, via Muroni 23/a, 07100 Sassari, Italy;* [b]*Laboratorio MOSE, Dipartimento di Ingegneria Chimica, dell'Ambiente e delle Materie Prime, Università degli Studi di Trieste, Piazzale Europa 1, 34127 Trieste, Italy;* [c]*Dipartimento di Scienze e Tecnologie Biomediche, Sezione di Microbiologia e Virologia Generale e Biotecnologie Microbiche, Università degli Studi di Cagliari, Cittadella Universitaria, 09042 Monserrato (Cagliari), Italy*

Abstract: A series N-[4-(1*H*(2*H*)-benzotriazol-1(2)-yl)phenyl]alkylcarboxamides (**8e-k**, **9e-i, k, l**) and their parent amines (**5a-c** and **6a-d**) were prepared according to Schemes (**1** and **2**). Compounds were evaluated *in vitro* for cytotoxicity and antiviral activity against a wide spectrum of RNA (positive- and negative-sense) viruses, like [Bovine Viral Diarrhea Virus (BVDV), Yellow Fever Virus (YFV), Coxsackie Virus B (CVB-2), Polio Virus (Sb-1), Human Immunodeficiency Virus (HIV-1), Respiratory Syncytial Virus (RSV)] or double-stranded (dsRNA) virus, like Reoviridae (Reo-1). The Entero (CVB-2 and Sb-1) were the only viruses inhibited by title compounds. In particular, two of them emerged for their selective, although not very potent, antiviral activity: **8i**, which was the most active against CVB-2 (CC_{50} >100 μM; EC_{50} = 10 μM) and **9l**, which was the most active against Sb-1 (CC_{50} 90 μM; EC_{50} = 30 μm). Title compounds were evaluated *in silico* against the Sb-1 helicase, as the crystal structure of this enzyme was not available, the corresponding 3D model was obtained by homology techniques (see Fig. **2**).

Key Words: Benzotriazolylphenylcarboxamides, Anti-viral activity, Picornaviridae, Cytotoxicity, SAR, Polio virus (Sb-1) helicase, *in silico* evaluation.

INTRODUCTION

The study of the biological properties of benzotriazoles was first started by Sparatore *et al.* [1-2], who described the interesting pharmacological activities of derivatives bearing substituents at positions 1 or 2 [3-8]. Being involved in a collaboration with the Sparatore team [3,6,7,9-11], we then developed a separate chemistry and further investigated the biological potential of benzotriazoles [12-16]. In particular, we described several 3-aryl-benzotriazol-1(2)-yl-acrilonitriles, which were found to be endowed with antitubercular activity [17-20] partly retained by the corresponding amides and carboxylic acids [18]. In addition, we described 3-aryl-benzotriazol-(1)-yl-acrilonitriles, which possess an interesting antiproliferative activity [19-20]. This confirmed that the bioisosteric replacement of a benzimidazole with a benzotriazole nucleus leads to novel biological activities.

In this context we have now prepared a series of benzotriazol-1(2)-yl-phenylamino derivatives, summarized in Fig. (**1**).

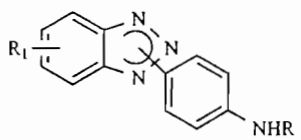

R_1 = H, 5,6-*di*CH_3, 5(6)-CF_3;
R = H, COalkyl.

Fig. (1). Novel benzotriazol-1(2)-yl-phenylamino derivatives.

The substituents in the benzo moiety of benzotriazoles (none, dimethyl or trifluoromethyl) and the acyl groups (acetic, propanoic or butanoic) linked to the amino group were chosen in order to evaluate the effect of both electron-releasing (dimethyl) and electron-withdrawing (trifluoromethyl) groups as well as both the lipophilic and steric hindrance (acetic, propanoic and butanoic) on the biological activity.

Title compounds were evaluated in cell-based assays for cytotoxicity and for antiviral activity against a wide spectrum of RNA viruses (positive- and negative-sense) [Bovine Viral Diarrhea Virus (BVDV), Yellow Fever Virus (YFV), Coxsackie Virus B (CVB-2), Polio Virus (Sb-1), Human Immunodeficiency Virus (HIV-1), Respiratory Syncytial Virus (RSV)] or double-stranded (dsRNA) virus, like Reoviridae (Reo-1).

CHEMISTRY

The benzotriazol-1(2)-ylphenylamino intermediates (**5a-c** and **6a-d**) were prepared, as reported in Scheme (**1**), by condensation of 4-chloro-nitrobenzene (**2**) with the appropriate

*Address correspondence to these authors at the Dipartimento Farmaco Chimico Tossicologico, Facoltà di Farmacia, Università di Sassari, *via* Muroni 23/a, 07100 Sassari, Italy; Tel: +39-079-228722; Fax: +39-079-228720; E-mail: acarta@uniss.it

Dipartimento di Scienze e Tecnologie Biomediche, Sezione di Microbiologia e Virologia Generale e Biotecnologie Microbiche, Università degli Studi di Cagliari, Cittadella Universitaria, 09042 Monserrato (Cagliari), Italy; E-mail: placolla@unica.it

1573-4064/06 $50.00+.00

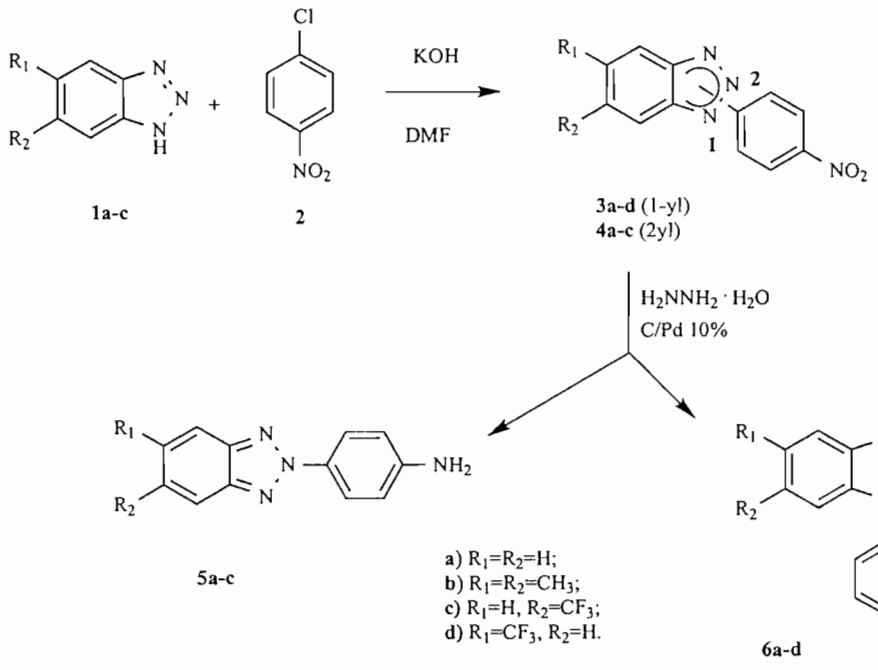

Scheme (1). Synthesis of intermediates (**5a-c** and **6a-d**).

benzotriazoles (**1a-c**) in DMF in the presence of KOH, to obtain a mixture of 1(2)-*p*nitrophenyl derivatives (**3a-d/4a-c**). The latter underwent reduction by hydrazine hydrate and 10% palladium-charcoal in refluxing ethanol, for 1 h. Chromatography on silica gel (eluent: diethyl ether-light petroleum 8:2) allowed the separation of the desired isomers **5a-c** and **6a-d**.

2-(4-Aminophenyl)benzimidazole (**10**) was prepared following the procedure previously described in the literature [21,22]. The final products **8e-k**, **9e-i,k,l** and **11** were prepared by condensation of the amino derivatives **5a-c**, **6a-d** and **10** with the appropriate anhydride (**7e-g**) under stirring at 100 °C for 2 h (Scheme **2**).

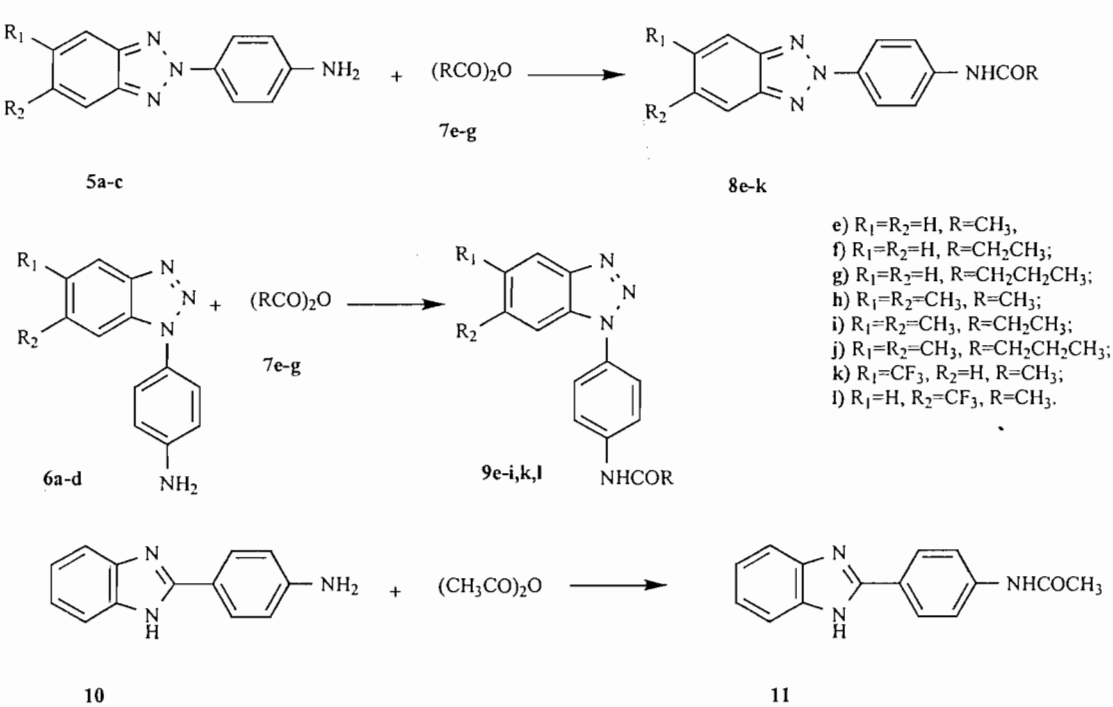

Scheme (2). Synthesis of N-[4-(1*H*(2*H*)-benzotriazol-1(2)-yl)phenyl]alkylcarboxamides (**8e-k** and **9e-i,k,l**) and N-[4-(2*H*-benzimidazol-2-yl)phenyl]acetylcarboxamide (**11**).

VIROLOGY

Title compounds (**5a-c**, **6a-d**, **8e-k**, **9e-i,k,l** and **11**) were evaluated *in vitro* against viruses representative of two of the three genera of the Flaviviridae family, i.e. *Flaviviruses* (Yellow Fever Virus YFV) and *Pestiviruses* (Bovine Viral Diarrhea Virus BVDV), as *Hepaciviruses* do not replicate in cell cultures. Compounds were also tested against representatives of other virus families containing a single-stranded RNA genome, either positive sense (ssRNA$^+$), like Picornaviridae [Coxsackie B2 (CVB-2) and Polio (Sb-1)] and Retroviridae [Human Immunodeficiency Virus (HIV-1)], or negative sense (ssRNA$^-$), like Paramyxoviridae [Respiratory Syncytial Virus (RSV)]. Representatives of double-stranded RNA [Reo-1] were also tested.

MOLECULAR MODELING

Title compounds (**5a-c**, **6a-d**, **8e-k**, **9e-i,k,l** and **11**) were also evaluated *in silico* against the Polio virus (Sb-1) helicase. As the crystal structure of this enzyme was not available, the corresponding 3D model was obtained by homology techniques (see Fig. **2**). The compounds were modeled and docked into the protein, as exemplified by compound **9l** in Fig. (**3a-c**), and the corresponding free energies of binding were calculated using molecular dynamics simulations (see Table **3**).

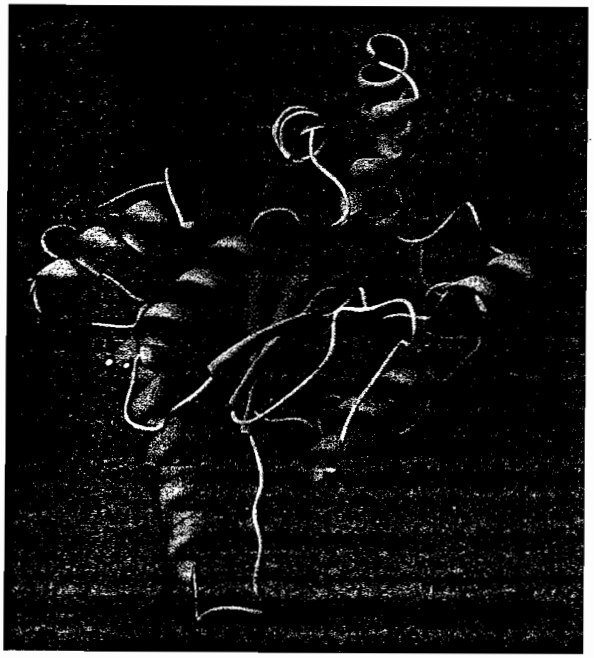

Fig. (2). Three-dimensional model of the Polio (Sb-1) helicase. Colour code for secondary structural motifs: helices: green; β-sheets: gold; turns and coils: cyan.

RESULTS AND DISCUSSION

Benzotriazol-1(2)-ylphenylamino derivatives (**5a-c** and **6a-d**), N-[4-(1H(2H)-benzotriazol-1(2)-yl)phenyl]alkylcarboxamides (**8e-k** and **9e-i,k,l**) and N-[4-(2*H*-benzimidazol-2-yl)phenyl]acetylcarboxamide (**11**) were evaluated in parallel cell-based assays for cytotoxicity (Table **1**) and antiviral activity (Table **2**).

As far as the cytotoxicity is concerned, only compound **5c** was moderately cytotoxic for cells grown in confluent monolayers (MDBK, BHK and Vero) as well as in suspension cultures (MT-4). All the other compounds were, in general, slightly more cytotoxic for the latter. The likely reason for this phenomenon is that MT-4 cells are grown under conditions allowing exponential growth (which is a prerequisite for HIV replication), whereas cells in confluent monolayers are non-dividing cultures.

When evaluated for antiviral activity, compounds **6a**, **8e**, **8i**, **8j**, **9g**, **9h** and **9i** exhibited EC_{50}s lower than 50 μM against CVB-2, with **8i** displaying the most potent activity (EC_{50} = 10 μM) together with low cytotoxicity (CC_{50} > 100 μM). Compounds **5a**, and **9l** exhibited EC_{50}s lower than 50 μM against Sb-1, whereas compounds **6b** and **8f** were active against both CVB-2 and Sb-1. None of the compounds protected the cells from the cytopathogenicity induced by the other ssRNA$^+$ and by the dsRNA representative. Interestingly, compound **8j** exhibited moderate activity (EC_{50} = 70 μM) against RSV, the RNA$^-$ representative.

Structure activity relationships suggest that the potent activity of **8i** is probably due to the presence of methyl groups at positions 5 and 6, of a phenyl group at position 2 and of a propanoyl-amide at 4'. Replacement of propanoyl with butanoyl (compound **8j**) leads to a slight decreases of activity against CVB-2 (EC_{50} = 30 μM), to an increase of potency against Sb-1 (EC_{50} = 53 μM) and RSV (EC_{50} = 70 μM), and to no change in cytotoxicity (CC_{50} > 100 μM). In the case of the anti-Sb-1 activity, a CF_3 group at position 6, a phenyl at position 1 and an acetyl substituent at the amidic group (compound **9l**) correlates with the highest potency (EC_{50} = 30 μM). Replacement of CF_3 with a methyl group at positions 5 and 6 essentially maintains unaltered the activity against Sb-1 while increasing that against CVB-2, independently from the substituent on the nitrogen atom (compounds **6b**, **9h**, **9i**). However, the cytotoxicity of the compounds of series **9** (benzotriazol-1-yl derivatives) is, in general, much higher than that of the compounds of series **8** (benzotriazol-2- yl derivatives). In the light of the observed activity of the latter series of benzotriazoles and of antiviral activities of several benzimidazole derivatives recently reported [23-25] we decided to investigate whether reverting one of our compounds to a benzimidazole could lead to maintaining the activity unaltered.

Compound (**11**) was purposely prepared and its activity in the above tests was completely negative. This supports the suggestion that sometimes this bioisosteric replacement is not reversible.

According to the procedure adopted, all compounds were characterized by a similar docking mode in the putative binding site of the Polio (Sb-1) helicase, as exemplified by compound **9l** in Fig. (**3a**). The portion of the enzyme making up the binding site interacting with the inhibitors consist of two loops, part of two β-sheets, and part of three helices (see Fig. **3b**). In particular, the residues lining the pocket (see Fig. **3c**)

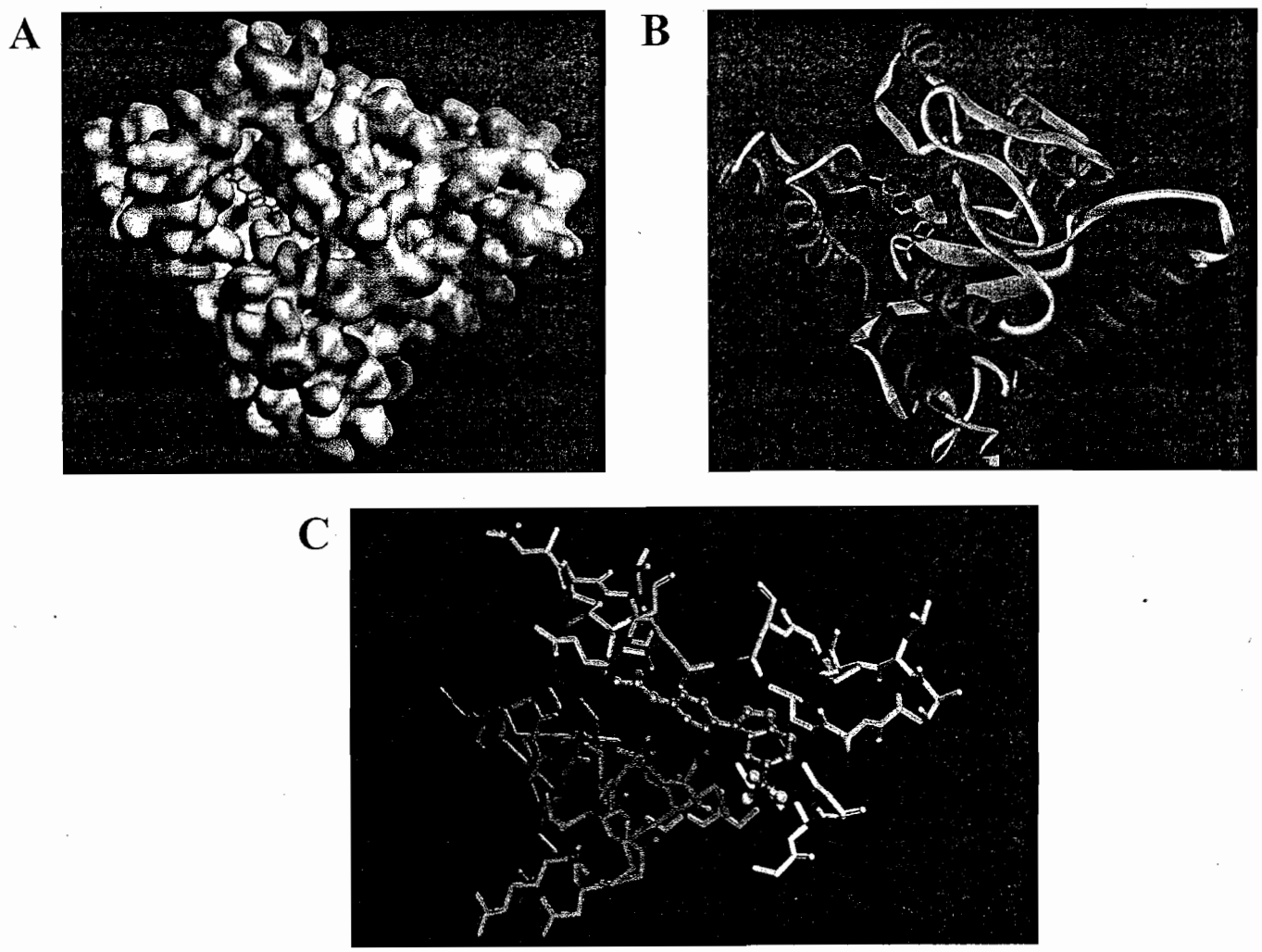

Fig. (3). A. Binding of compound **9l** to the putative binding site on the surface of Polio (Sb-1) helicase. **B**. Cartoon of the binding mode of compound **9l** in the putative binding site of the Polio (Sb-1) helicase. Compound **9l** is in atom-coloured stick representation. Enzyme secondary structure motifs are coloured as follows: helices: red; b-sheets: cyan; loops and turns: green and white. **C**. Equilibrated molecular dynamics snapshot of the docked compound **9l** in the putative binding site of Polio (Sb-1) helicase. Compound **9l** is shown in atom-coloured ball-and-stick. The amino acids are colour-coded as follows: first loop (residues Asp176–Pro182): pink; second loop (residues Ser156-Asp160): yellow; first β-sheet (residues Ala220-Thr222): cyan; second b-sheet (residues Gly129-Ser130): green; helix 1 (residues (residues Ser296-Ser302): red; helix 2 (residues Gly134-Ser136): white; helix 3 (residues Arg256-Ala265): blue. For the sake of clarity, water molecules and hydrogen atoms are omitted.

include the side chains of residues from Asp176 to Pro 182 in the first loop (pink), and those of residues from Ser156 to Asp160 of the second loop (yellow). Amino acids Ala220, Ser221, and Thr222 (cyan), and residues Gly129 and Ser130 (green) contribute to binding from the two β-sheet portions, respectively. Finally, the portion of helix 1 involved spans from Ser296 to Ser302 (red), whilst helix 2 and helix 3 concur with residues from Gly134 to Ser136 (white) and from Arg256 to Ala265 (blue), respectively.

Further insights into the forces involved in substrate binding can be obtained by analyzing the free energy components, which are listed in Table (**3**) for all title compounds.

As we may see from this Table, both the intermolecular van der Waals and the electrostatics are important contributions to the binding. Comparing the van der Waals/non polar ($\Delta E_{vdW} + \Delta G_{NP}$) with the electrostatic contributions ($\Delta E_{EL} + \Delta G_{PB}$) for all molecules, however, we see that in all cases the association between inhibitors and the target protein is mainly driven by more favourable nonpolar interactions in the complex than in solution. Quite generally, electrostatics disfavour the docking of ligand and receptor molecules because of the unfavourable change in the electrostatics of solvation is mostly, but not fully, compensated by the favourable electrostatics within the resulting ligand-receptor complex. Indeed, the total electrostatic energy contributions ($\Delta E_{EL} + \Delta G_{sol}$) for all helicase/benzotriazole derivatives complex formations are unfavourable, the **9l**/helicase complex formations being less unfavourable of the entire series because of a less positive total electrostatic term in which the penalty paid by the electrostatics of solvation is better compensated by favourable electrostatic interactions within the

Table 1. Cytotoxicity of 5a-c, 6a-d, 8e-k, 9e-i,k,l and 11

Compds	Cell lines			
	[a]CC_{50}			[b]CC_{50}
	[c]MDBK	[d]BHK	[e]Vero	[f]MT-4
5a	83	>100	60	>100
5b	>100	>100	>100	90
5c	32	36	30	25
6a	>100	>100	>100	>100
6b	>100	>100	>100	57
6c	>100	>100	74	60
6d	70	>100	87	45
8e	61	>100	71	100
8f	82	>100	>100	57
8g	>100	>100	>100	>100
8h	>100	>100	>100	>100
8i	>100	>100	>100	>100
8j	>100	>100	>100	>100
8k	>100	>100	80	>100
9e	>100	>100	>100	>100
9f	>100	>100	>100	>100
9g	>100	>100	>100	100
9h	>100	>100	≥100	48
9i	>100	>100	≥100	49
9k	93	>100	50	>100
9l	>100	>100	90	55
11	>100	>100	>100	>100

[a]Compound concentration (μM) required to reduce the viability of mock-infected cells by 50%, as determined by the MTT method, or the confluency of the monolayer (Vero), as determined by methylene blue staining.

[b]Compound concentration (μM) required to reduce cell proliferation by 50%, as determined by the MTT method, under conditions allowing untreated controls to undergo at least three consecutive rounds of multiplication. Data represent mean values for three independent determinations. Variation among duplicate samples was less than 15%.

[c]Madin Darby Bovine Kidney; [d]Baby Hamster Kidney; [e]Monkey Kidney; [f]$CD4^+$ human T-cells.

complex. Thus, even though electrostatics destabilizes each complex formation, it is the optimized balance of opposing electrostatic contributions that leads to tighter binding (see Table 3).

CONCLUSIONS

In the light of the above mentioned results, we conclude that title compounds are, in general, endowed with good activity against the Entero viruses. Compounds **8i** and **9l** resulted the most potent against CVB-2 and Sb-1, respectively and might represent new interesting leads. Molecular dynamics simulations on title compounds/Polio helicase complexes have shown to be able to rank binding affinities of all inhibitors, to provide insight into the interactions occurring in the active site, and the origins of variations in the corresponding binding free energy. Accordingly, the computational strategy used in this paper can provide a blueprint for new inhibitors in structure-based drug design or in predicting binding affinity of a ligand prior to new organic synthesis.

EXPERIMENTAL SECTION

Chemistry

M.p.s were uncorrected and were taken in open capillaries in a Digital Electrothermal IA9100 melting point apparatus. ^1H NMR spectra were recorded on a Varian XL-200 (200 MHz) instrument, using TMS as internal standard. The

Table 2. Activity of 5a-c, 6a-d, 8e-k, 9e-i,k,l and 11 Against the RNA Viruses Infecting the Indicated Cell Lines

Genome	ssRNA$^+$					dsRNA	ssRNA$^-$
Genus Cell line	Pesti MDBK	Flavi BHK	Entero Vero		Retro MT-4	Reo BHK	Paramyxo Vero
Virus	BVDV	YFV	CVB-2	Polio-1	HIV-1	Reo-1	RSV
Compds	^{a}EC$_{50}$	^{b}EC$_{50}$	^{b}EC$_{50}$		^{a}EC$_{50}$	^{b}EC$_{50}$	^{b}EC$_{50}$
5a	>83	>100	>60	42	>100	>100	>60
5b	>100	>100	>100	>100	>90	>100	>100
5c	>32	>36	>30	>30	>25	>100	>30
6a	>100	>100	49	>100	>100	>100	>100
6b	>100	>100	39	38	>57	>100	>100
6c	>100	>100	>74	>74	>60	>100	>74
6d	>70	>100	>87	>87	>45	>100	>87
8e	>61	>100	28	>71	>100	>100	>71
8f	>82	>100	30	47	>57	>100	>100
8g	>100	>100	>100	>100	>100	>100	>100
8h	>100	>100	>100	>100	>100	>100	>100
8i	>100	>100	10	>100	>100	>100	>100
8j	>100	>100	30	53	>100	>100	70
8k	>100	>100	>80	>80	>100	>100	>80
9e	>100	>100	83	>100	>100	>100	>100
9f	>100	>100	62	87	>100	>100	>100
9g	>100	>100	44	87	>100	>100	>100
9h	>100	>100	31	59	>48	>100	>100
9i	>100	>100	32	51	>49	>100	>100
9k	>93	>100	>50	>50	>100	>100	>50
9l	>100	>100	>90	30	>55	>100	>90
11	>100	>100	>100	>100	>100	72	>100

^{a}Compound concentration (μM) required to achieve 50% protection from virus-induced cytopathogenicity, as determined by the MTT method.

^{b} Compound concentration (μM) required to reduce the virus plaque number by 50%.

chemical shift values are reported in ppm (δ) and coupling constants (*J*) in Hertz (Hz). Signal multiplicities are represented by: s (singlet), d (doublet), dd (double doublet), t (triplet), q (quadruplet) and m (multiplet). MS spectra were performed on a combined HP 5790 (GC)-HP 5970 (MS) apparatus. Column chromatography was performed using 70-230 mesh (Merck silica gel 60). Light petroleum refers to the fraction with b.p. 40-60 °C. The progress of the reactions, the R_f and the purity of the final compounds were monitored by TLC using Merck F-254 commercial plates. Analyses indicated by the symbols of the elements were within ± 0.4 % of the theoretical values.

Starting Materials and Intermediates

Benzotriazole (**1a**), 5,6-dimethylbenzotriazole (**1b**), 4-chloro-nitrobenzene (**2**), acetic anhydride (**7c**), propionic anhydride (**7d**) and butyril anhydride (**7e**) were commercially available, 5-trifluoromethylbenzotriazole (**1c**) was prepared following the procedure previously described by Paglietti [9], 2-(4-aminophenyl)benzimidazole (**10**) was prepared following the procedure previously described [21-22]. 2-(4-aminophenyl)benzotriazole (**5a**), 1-(4-aminophenyl)benzotriazole (**6a**), 2-(4-aminophenyl)-5,6-dimethylbenzotriazole (**5b**), 1-(4-aminophenyl)-5,6-dimethylbenzotriazole (**6b**), 2-(4-aminophenyl)-5-trifluoromethylbenzotriazole (**5c**), 1-(4-

Table 3. **Free Energy Components and Total Binding Free Energies for Title Compounds and Polio (Sb-1) Helicase**

Compd	ΔE_{vdw}	ΔE_{EL}	ΔE_{MM}	ΔG_{PB}	ΔG_{NP}	ΔG_{solv}	$T\Delta S$	$\Delta G_{calc.}$
5a	-49.7	-31.3	-81.0	55.4	-6.4	49.0	15.2	-16.8
5b	-48.0	-29.0	-77.0	57.2	-6.0	51.2	15.9	-10.0
5c	-47.1	-31.6	-78.7	60.0	-6.2	53.8	17.3	-7.6
6a	-38.2	-27.0	-65.2	50.6	-6.8	43.7	12.9	-8.5
6b	-41.2	-27.1	-68.3	49.8	-6.9	42.9	11.5	-13.9
6c	-40.0	-25.0	-65.0	51.2	-6.7	44.5	13.4	-7.2
6d	-38.8	-25.6	-64.4	52.0	-6.7	45.3	13.6	-5.5
8c	-44.2	-29.1	-73.3	58.3	-6.2	52.1	16.5	-4.7
8f	-48.2	-33.4	-81.6	56.3	-6.3	50.0	15.7	-16.0
8g	-43.9	-30.7	-74.6	58.3	-6.1	52.2	16.6	-5.8
8h	-45.3	-29.1	-74.4	57.5	-6.1	51.3	16.1	-7.0
8i	-44.9	-30.2	-75.1	57.5	-6.3	51.2	16.1	-7.8
8j	-45.9	-32.9	-78.8	55.9	-6.4	49.5	15.8	-13.5
8k	-46.8	-29.0	-75.8	58.7	-6.2	52.5	17.0	-6.4
9e	-37.1	-27.0	-64.2	51.5	-7.0	44.5	12.3	-7.3
9f	-38.3	-28.0	-66.4	51.0	-6.7	44.3	13.1	-9.0
9g	-40.4	-26.3	-66.7	50.7	-6.8	43.9	13.1	-9.8
9h	-41.3	-25.9	-67.2	48.6	-6.6	41.9	12.1	-13.2
9i	-41.9	-27.2	-69.1	49.3	-6.6	42.8	11.5	-14.9
9k	-40.0	-24.5	-64.4	51.2	-6.7	44.5	13.9	-6.0
9l	-41.7	-29.3	-71.0	48.7	-6.9	41.8	12.9	-16.3
11	-44.4	-28.5	-72.9	58.0	-6.3	51.7	16.8	-4.5

aminophenyl)-6-trifluoromethylbenzotriazole (**6c**) and 1-(4-aminophenyl)-5-trifluoromethylbenzotriazole (**6d**), were prepared following the procedure below described.

Preparation of the Intermediates 1(2)-(4-aminofenyl)benzotriazoles (5a-c and 6a-d)

To a stirred solution of benzotriazole (**1a**), 5,6-dimethylbenzotriazole (**1b**) or 5-trifluoromethylbenzotriazole (**1c**) (42 mmol) and KOH (2.6 g, 46 mmol) in DMF (60 mL), a solution of 4-chloro-nitrobenzene (**2**) (7.0 g, 47 mmol) in DMF (15 mL), was slowly added dropwise. After the addition was complete, the reaction mixture was heated at 110 °C and the stirring was continued for an additional 23 h. On cooling to r.t., the mixture reaction afforded, directly or after dilution by water, a crude precipitate that filtered off, washed with water and dried, afforded the desired mixtures **3a/4a** (76% yield), **3b/4b** (80% yield) and **3c/3d/4c** (60% yield) from **1a**, **1b** and **1c** respectively. Thus, a suspension of the mixture **3a/4a**, **3b/4b** or **3c/3d/4c** (28 mmol), hydrazine hydrate (98%, 13 mL) and 10% palladium-charcoal (0.6 g) in ethanol (100 mL) was refluxed for 1 h. On cooling to r.t., the catalyst was filtered off and the solvent and the excess of hydrazine was removed *in vacuo*. The resulting crude residue was chromatographed on silica gel (eluent: diethyl ether-light petroleum 8:2), affording in sequence **5a** and **6a** (from reduction of **3a/4a**), **5b** and **6b** (from reduction of **3b/4b**), **5c**, **6c** and **6d** (from reduction of **3c/3d/4c**) (Scheme **1**). Melting points, yields, analytical and spectroscopical data are reported below.

2-(4-aminophenyl)benzotriazole (5a)

This compound was obtained in 25% of total yield; m.p. 166-167 °C (diethyl ether); TLC (diethyl ether-light petroleum 7:3): R_f 0.49; IR (nujol): ν 3380, 3340, 1625, 1600 cm^{-1}; UV (EtOH): λ_{max} 342, 208 nm; ^1H NMR ($CDCl_3$): δ 8.13 (dd, 2H, J = 9.0 and 2.2 Hz, H-2' + H-6'), 7.91 (m, 2H, H-4 + H-7), 7.39 (m, 2H, H-5 + H-6), 6.80 (dd, 2H, J = 9.0 and 2.2 Hz, H-3' + H-5'), 3.92 (s, 2H, NH_2). MS: *m/z* 210 (M^+). Anal. $C_{12}H_{10}N_4$ (C, H, N).

1-(4-aminophenyl)benzotriazole (6a)

This compound was obtained in 40% of total yield; m.p. 132-133 °C (diethyl ether); TLC (diethyl ether-light petroleum 7:3): R_f 0.24; IR (nujol): ν 3500-3350, 1630, 1600 cm^{-1}; UV (EtOH): λ_{max} 301, 254, 205 nm; ^1H NMR ($CDCl_3$): δ 8.12 (d, 1H, *J* = 8.2 Hz, H-4), 7.66 (d, 1H, *J* = 8.2 Hz, H-7), 7.55-7.37 (m, 4H, H-5 + H-6 + H-2' + H-6'), 6.88 (dd, 2H, *J* = 8.6 and 2.0 Hz, H-3' + H-5'), 3.70 (s, 2H, NH_2). MS: *m/z* 210 (M^+). Anal. $C_{12}H_{10}N_4$ (C, H, N).

2-(4-aminophenyl)-5,6-dimethylbenzotriazole (5b)

This compound was obtained in 24% of total yield; m.p. 218-219 °C (diethyl ether); TLC (light petroleum-ethyl acetate 7:3): R_f 0.40; IR (nujol): ν 3400-3350, 1625 cm^{-1}; UV (EtOH): λ_{max} 244, 208 nm; ^1H NMR ($CDCl_3$): δ 8.08 (dd, 2H, *J* = 8.8 and 2.0 Hz, H-2' + H-6'), 7.63 (s, 2H, H-4 + H-7), 6.79 (dd, 2H, *J* = 8.8 and 2.0 Hz, H-3' + H-5'), 3.85 (s, 2H, NH_2), 2.41 (s, 6H, 2 CH_3). MS: *m/z* 238 (M^+). Anal. $C_{14}H_{14}N_4$ (C, H, N).

1-(4-aminophenyl)-5,6-dimethylbenzotriazole (6b)

This compound was obtained in 36% of total yield; m.p. 169-170 °C (diethyl ether); TLC (light petroleum-ethyl acetate 7:3):R_f 0.23; IR (nujol): ν 3450, 3300, 1625 cm^{-1}; UV (EtOH): λ_{max} 303, 255, 204 nm; ^1H NMR ($CDCl_3$): δ 7.83 (s, 1H, H-4), 7.48 (dd, 2H, *J* = 8.8 and 2.2 Hz, H-2' + H-6'), 7.40 (s, 1H, H-7), 6.85 (dd, 2H, *J* = 8.8 and 2.2 Hz, H-3' + H-5'), 3.95 (s, 2H, NH_2), 2.42 (s, 6H, 2 CH_3). MS: *m/z* 238 (M^+). Anal. $C_{14}H_{14}N_4$ (C, H, N).

2-(4-aminophenyl)-5-trifluoromethylbenzotriazole (5c)

This compound was obtained in 25% of total yield; m.p. 132-133 °C (diethyl ether); TLC (light petroleum-ethyl acetate 6:4):R_f 0.54; IR (nujol): ν 3200-3100 cm^{-1}; UV (EtOH): λ_{max} 352, 240, 212 nm; ^1H NMR ($CDCl_3$): δ 8.25 (s, 1H, H-4), 8.15 (d, 2H, *J* = 9.0 Hz, H-2' + H-6'), 8.02 (d, 1H, *J* = 9.0 Hz, H-6), 7.58 (d, 1H, *J* = 9.0 Hz, H-7), 6.82 (d, 2H, *J* = 9.0 Hz, H-3' + H-5'), 4.00 (s, 2H, NH_2). MS: *m/z* 278 (M^+). Anal. $C_{13}H_9N_4F_3$ (C, H, N).

1-(4-aminophenyl)-6-trifluoromethylbenzotriazole (6c)

This compound was obtained in 6% of total yield; m.p. 83-84 °C (diethyl ether); TLC (light petroleum-ethyl acetate 6:4):R_f 0.36; IR (nujol): ν 3200-3100 cm^{-1}; UV (EtOH): λ_{max} 306, 254, 208 nm; ^1H NMR ($CDCl_3$): δ 8.25 (d, 1H, *J* = 8.6 Hz, H-5), 7.95 (s, 1H, H-7), 7.65 (d, 1H, *J* = 8.6 Hz, H-4), 7.48 (d, 2H, *J* = 8.6 Hz, H-2' + H-6'), 6.88 (d, 2H, *J* = 9.0 Hz, H-3' + H-5'), 4.03 (s, 2H, NH_2). MS: *m/z* 278 (M^+). Anal. $C_{13}H_9N_4F_3$ (C, H, N).

1-(4-aminophenyl)-5-trifluoromethylbenzotriazole (6d)

This compound was obtained in 8% of total yield; m.p. 94-95 °C (diethyl ether); TLC (light petroleum-ethyl acetate 6:4):R_f 0.20; IR (nujol): ν 3260-3100 cm^{-1}; UV (EtOH): λ_{max} 304, 256, 205 nm; ^1H NMR ($CDCl_3$): δ 8.44 (s, 1H, H-4), 7.79-7.72 (m, 2H, H-6 + H-7), 7.48 (d, 2H, *J* = 8.4 Hz, H-2' + H-6'), 6.87 (d, 2H, *J* = 8.6 Hz, H-3' + H-5'), 4.01 (s, 2H, NH_2). MS: *m/z* 278 (M^+). Anal. $C_{13}H_9N_4F_3$ (C, H, N).

General Procedure for Preparation of N-[4-(1*H*(2*H*)-benzotriazol-1(2)-yl)phenyl]alkylcarboxamides (8e-k and 9e-i,k,l) and N-[4-(2*H*-benzimidazol-2-yl)phenyl]acetylcarboxamide (11)

A stirred suspension of the aminophenylbenzotriazole derivative (**5a-c**, **6a-d**) or 2-(4-aminophenyl)benzimidazole (**10**) (1.5 mmol) in the appropriate anhydride (**7e-g**) (3 mL), was heated to 100 °C for 2 h. On cooling to r.t., the resulting precipitate was filtered off, washed with water and dried, to afford the desired amides **8e-k**, **9e-i,k,l** and **11** (Scheme **2**). Melting points, yields, analytical and spectroscopical data are reported below.

N-[4-(2*H*-benzotriazol-2-yl)phenyl]acetylcarboxamide (8e)

This compound was obtained in 67% yield; m.p. 192-193 °C (diethyl ether); TLC (diethyl ether-light petroleum 7:3): R_f 0.33; IR (nujol): ν 3250, 1660, 1610 cm^{-1}; UV (EtOH): λ_{max} 323, 264, 254, 202 nm; ^1H NMR ($CDCl_3$ + DMSO-d_6): δ 8.31 (dd, 2H, *J* = 9.0 and 2.0 Hz, H-2' + H-6'), 7.92 (m, 2H, H-4 + H-7), 7.72 (dd, 2H, *J* = 9.0 and 2.2 Hz, H-3' + H-5'), 7.45 (s, 1H, NH), 7.42 (m, 2H, H-5 + H-6), 2.23 (s, 3H, CH_3). MS: *m/z* 252 (M^+). Anal. $C_{14}H_{12}N_4O$ (C, H, N).

N-[4-(2*H*-benzotriazol-2-yl)phenyl]propionylcarboxamide (8f)

This compound was obtained in 60% yield; m.p. 191-192 °C (diethyl ether); TLC (diethyl ether-light petroleum 7:3): R_f 0.36; IR (nujol): ν 3250, 1665, 1610 cm^{-1}; UV (EtOH): λ_{max} 324, 264, 255, 203 nm; ^1H NMR ($CDCl_3$): δ 8.31 (dd, 2H, *J* = 9.0 and 2.0 Hz, H-2' + H-6'), 7.92 (m, 2H, H-4 + H-7), 7.74 (dd, 2H, *J* = 9.0 and 2.0 Hz, H-3' + H-5'), 7.42 (m, 2H, H-5 + H-6), 7.38 (s, 1H, NH), 2.45 (q, 2H, *J* = 7.6 Hz, CH_2), 1.28 (t, 3H, *J* = 7.6 Hz, CH_3). MS: *m/z* 266 (M^+). Anal. $C_{15}H_{14}N_4O$ (C, H, N).

N-[4-(2*H*-benzotriazol-2-yl)phenyl]butyrilcarboxamide (8g)

This compound was obtained in 75% yield; m.p. 224-225 °C (diethyl ether); TLC (diethyl ether-light petroleum 7:3): R_f 0.44; IR (nujol): ν 3300, 1670, 1600 cm^{-1}; UV (EtOH): λ_{max} 324, 264, 255, 202 nm; ^1H NMR ($CDCl_3$): δ 8.32 (dd, 2H, *J* = 9.0 and 2.0 Hz, H-2' + H-6'), 7.92 (m, 2H, H-4 + H-7), 7.74 (dd, 2H, *J* = 9.0 and 2.2 Hz, H-3' + H-5'), 7.42 (m, 2H, H-5 + H-6), 7.31 (s, 1H, NH), 2.40 (t, 2H, *J* = 7.2 Hz, $COCH_2$), 1.80 (m, 2H, CH_2CH_3), 1.04 (t, 3H, *J* = 7.4 Hz, CH_2CH_3). MS: *m/z* 280 (M^+). Anal. $C_{16}H_{16}N_4O$ (C, H, N).

N-[4-(5,6-dimethyl-2*H*-benzotriazol-2-yl)phenyl]acetylcarboxamide (8h)

This compound was obtained in 83% yield; m.p. 262-263 °C (acetone/diethyl ether); TLC (light petroleum-ethyl acetate 1:1): R_f 0.21; IR (nujol): ν 3250, 1680, 1610 cm^{-1}; UV (EtOH): λ_{max} 328, 258, 202 nm; ^1H NMR ($CDCl_3$): δ 8.27 (d, 2H, *J* = 8.8 Hz, H-2' + H-6'), 7.69 (d, 2H, *J* = 8.8 Hz, H-3' + H-5'), 7.64 (s, 2H, H-4 + H-7), 7.03 (s, 1H, NH), 2.42 (s,

6H, C_5-CH_3 + C_6-CH_3), 2.23 (s, 3H, $COCH_3$). MS: *m/z* 280 (M^+). Anal. $C_{16}H_{16}N_4O$ (C, H, N).

N-[4-(5,6-dimethyl-2*H*-benzotriazol-2-yl)phenyl]propionylcarboxamide (8i)

This compound was obtained in 71% yield; m.p. 245-246 °C (acetone/diethyl ether); TLC (light petroleum-ethyl acetate 1:1): R_f 0.49; IR (nujol): ν 3300, 1700, 1600 cm^{-1}; UV (EtOH): λ_{max} 328, 258, 204 nm; ^1H NMR ($CDCl_3$ + DMSO-d_6): δ 10.04 (s, 1H, NH), 8.17 (d, 2H, *J* = 8.8 Hz, H-2' + H-6'), 7.84 (d, 2H, *J* = 8.8 Hz, H-3' + H-5'), 7.63 (s, 2H, H-4 + H-7), 2.42 (s, 6H, C_5-CH_3 + C_6-CH_3), 2.40 (q, 2H, *J* = 7.6 Hz, CH_2CH_3), 1.19 (t, 3H, *J* = 7.6 Hz, CH_2CH_3). MS: *m/z* 294 (M^+). Anal. $C_{17}H_{18}N_4O$ (C, H, N).

N-[4-(5,6-dimethyl-2*H*-benzotriazol-2-yl)phenyl]butyrilcarboxamide (8j)

This compound was obtained in 92% yield; m.p. 225-227 °C (chloroform); TLC (diethyl ether-light petroleum 8:2): R_f 0.15; IR (nujol): ν 3300, 1680, 1600 cm^{-1}; UV (EtOH): λ_{max} 300, 260, 206 nm; ^1H NMR ($CDCl_3$): δ 8.26 (d, 2H, *J* = 9.0 Hz, H-2' + H-6'), 7.71 (d, 2H, *J* = 9.0 Hz, H-3' + H-5'), 7.64 (s, 2H, H-4 + H-7), 7.31 (s, 1H, NH), 2.42 (s, 6H, C_5-CH_3 + C_6-CH_3), 2.38 (t, 2H, *J* = 7.4 Hz, $COCH_2$), 1.80 (m, 2H, CH_2CH_3), 1.03 (t, 3H, *J* = 7.4 Hz, CH_2CH_3). MS: *m/z* 308 (M^+). Anal. $C_{18}H_{20}N_4O$ (C, H, N).

N-[4-(5-trifluoromethyl-2*H*-benzotriazol-2-yl)phenyl]acetylcarboxamide (8k)

This compound was obtained in 77% yield; m.p. 225-227 °C (acetone/diethyl ether); TLC (diethyl ether- ethyl acetate 1:1): R_f 0.29; IR (nujol): ν 3100, cm^{-1}; UV (EtOH): λ_{max} 326, 266, 256, 210 nm; ^1H NMR ($CDCl_3$): δ 8.34 (d, 2H, *J* = 9.0 Hz, H-2' + H-6'), 8.28 (s, 1H, H-4), 8.04 (d, 1H, *J* = 9.0 Hz, H-6), 7.75 (d, 2H, *J* = 9.0 Hz, H-3' + H-5'), 7.59 (d, 1H, *J* = 9.0 Hz, H-7), 7.38 (s, 1H, NH), 2.25 (s, 3H, CH_3). MS: *m/z* 320 (M^+). Anal. $C_{15}H_{11}N_4F_3O$ (C, H, N).

N-[4-(1*H*-benzotriazol-1-yl)phenyl]acetylcarboxamide (9e)

This compound was obtained in 63% yield; m.p. 197-198 °C (diethyl ether); TLC (diethyl ether-light petroleum 7:3): R_f 0.10; IR (nujol): ν 3080, 1690, 1610 cm^{-1}; UV (EtOH): λ_{max} 294, 259, 207 nm; ^1H NMR ($CDCl_3$ + DMSO-d_6): δ 10.06 (s, 1H, NH), 8.10 (d, 1H, *J* = 7.4 Hz, H-4), 7.92 (dd, 2H, *J* = 8.4 and 1.6 Hz, H-2' + H-6'), 7.78 (d, 1H, *J* = 7.4 Hz, H-7), 7.69 (dd, 2H, *J* = 8.4 and 1.6 Hz, H-3' + H-5'), 7.60 (dd, 1H, *J* = 8.2 and 7.2 Hz, H-6), 7.46 (dd, 1H, *J* = 8.2 and 7.2 Hz, H-5), 2.18 (s, 3H, CH_3). MS: *m/z* 252 (M^+). Anal. $C_{14}H_{12}N_4O$ (C, H, N).

N-[4-(1*H*-benzotriazol-1-yl)phenyl]propionylcarboxamide (9f)

This compound was obtained in 64% yield; m.p. 152-153 °C (diethyl ether); TLC (diethyl ether-light petroleum 7:3): R_f 0.19; IR (nujol): ν 3090, 1680, 1600 cm^{-1}; UV (EtOH): λ_{max} 295, 259, 208 nm; ^1H NMR ($CDCl_3$): δ 8.15 (d, 1H, *J* = 8.0 Hz, H-4), 7.84-7.71 (m, 5H, H-7 + 4 phenyl-H), 7.57 (dd, 1H, *J* = 8.0 and 7.2 Hz, H-6), 7.44 (dd, 1H, *J* = 8.0 and 7.2 Hz, H-5), 2.48 (q, 2H, *J* = 7.6 Hz, CH_2), 1.30 (t, 3H, *J* = 7.6 Hz, CH_3). MS: *m/z* 266 (M^+). Anal. $C_{15}H_{14}N_4O$ (C, H, N).

N-[4-(1*H*-benzotriazol-1-yl)phenyl]butyrilcarboxamide (9g)

This compound was obtained in 68% yield; m.p. 155-156 °C (diethyl ether); TLC (diethyl ether-light petroleum 7:3): R_f 0.25; IR (nujol): ν 3320, 1700, 1600 cm^{-1}; UV (EtOH): λ_{max} 295, 262, 208 nm; ^1H NMR ($CDCl_3$): δ 8.15 (d, 1H, *J* = 8.2 Hz, H-4), 7.84-7.71 (m, 5H, H-7 + 4 phenyl-H), 7.57 (dd, 1H, *J* = 8.2 and 7.4 Hz, H-6), 7.44 (dd, 1H, *J* = 8.2 and 7.4 Hz, H-5), 2.42 (t, 2H, *J* = 7.4 Hz, $COCH_2$), 1.82 (m, 2H, CH_2CH_3), 1.05 (t, 3H, *J* = 7.4 Hz, CH_2CH_3). MS: *m/z* 280 (M^+). Anal. $C_{16}H_{16}N_4O$ (C, H, N).

N-[4-(5,6-dimethyl-1*H*-benzotriazol-1-yl)phenyl]acetylcarboxamide (9h)

This compound was obtained in 75% yield; m.p. 185-186 °C (acetone/diethyl ether); TLC (light petroleum-ethyl acetate 1:1): R_f 0.16; IR (nujol): ν 3300, 1690, 1610 cm^{-1}; UV (EtOH): λ_{max} 299, 267, 204 nm; ^1H NMR ($CDCl_3$): δ 7.85 (s, 1H, H-4), 7.80-7.68 (m, 4H, 4 phenyl-H), 7.48 (s, 1H, H-7), 2.44 (s, 6H, C_5-CH_3 + C_6-CH_3), 2.26 (s, 3H, $COCH_3$). MS: *m/z* 280 (M^+). Anal. $C_{16}H_{16}N_4O$ (C, H, N).

N-[4-(5,6-dimethyl-1*H*-benzotriazol-1-yl)phenyl]propionylcarboxamide (9i)

This compound was obtained in 74% yield; m.p. 195-196 °C (acetone/diethyl ether); TLC (light petroleum-ethyl acetate 1:1): R_f 0.32; IR (nujol): ν 3270, 1690, 1610 cm^{-1}; UV (EtOH): λ_{max} 297, 268, 204 nm; ^1H NMR ($CDCl_3$): δ 7.86 (s, 1H, H-4), 7.82-7.69 (m, 4H, 4 phenyl-H), 7.48 (s, 1H, H-7), 2.47 (q, 2H, *J* = 7.6 Hz, CH_2CH_3), 2.43 (s, 6H, C_5-CH_3 + C_6-CH_3), 1.29 (t, 3H, *J* = 7.6 Hz, CH_2CH_3). MS: *m/z* 294 (M^+). Anal. $C_{17}H_{18}N_4O$ (C, H, N).

N-[4-(5-trifluoromethyl-1*H*-benzotriazol-1-yl)phenyl]acetylcarboxamide (9k)

This compound was obtained in 77% yield; m.p. 240-241 °C (acetone/diethyl ether); TLC (light petroleum-ethyl acetate 1:1): R_f 0.17; IR (nujol): ν 3150, cm^{-1}; UV (EtOH): λ_{max} 290, 258, 210 nm; ^1H NMR ($CDCl_3$ + DMSO-d_6): δ 10.16 (s, 1H, NH), 8.46 (s, 1H, H-4), 7.99-7.92 (m, 3H, H-6 + H-2' + H-6'), 7.83 (d, 1H, *J* = 9.0 Hz, H-7), 7.70 (d, 2H, *J* = 9.0 Hz, H-3' + H-5'), 2.17 (s, 3H, CH_3). MS: *m/z* 320 (M^+). Anal. $C_{15}H_{11}N_4F_3O$ (C, H, N).

N-[4-(6-trifluoromethyl-1*H*-benzotriazol-1-yl)phenyl]acetylylcarboxamide (9l).

This compound was obtained in 80% yield; m.p. 2001-202 °C (acetone/diethyl ether); TLC (light petroleum-ethyl acetate 1:1): R_f 0.26; IR (nujol): ν 3070, cm^{-1}; UV (EtOH): λ_{max} 300, 256, 207 nm; ^1H NMR ($CDCl_3$ + DMSO-d_6): δ 8.28 (d, 1H, *J* = 8.6 Hz, H-5), 8.02 (s, 1H, H-7), 7.84 (d, 2H, *J* = 8.8 Hz, H-2' + H-6'), 7.43-7.67 (m, 3H, H-6 + H-3' + H-5'), 7.47 (s, 1H, NH), 2.27 (s, 3H, CH_3). MS: *m/z* 320 (M^+). Anal. $C_{15}H_{11}N_4F_3O$ (C, H, N).

N-[4-(2*H*-benzimidazol-2-yl)phenyl]acetylcarboxamide (11)

This compound was obtained in 94% yield; m.p. >300 °C (acetone/diethyl ether); TLC (ethyl acetate-light petroleum 7:3): R_f 0.25; IR (nujol): ν 3250, 1675, 1605 cm^{-1}; UV (EtOH): λ_{max} 316, 258, 208 nm; ^1H NMR ($CDCl_3$ + DMSO-d_6): δ 10.09 (s, 1H, NH), 8.09 (d, 2H, *J* = 8.6 Hz, H-2' + H-6'), 7.75 (d, 2H, *J* = 8.6 Hz, H-3' + H-5'), 7.56 (dd, 2H, *J* = 7.0 and 2.0 Hz, H-4 + H-7), 7.19 (dd, 2H, *J* = 7.0 and 2.0 Hz, H-5 + H-6), 2.23 (s, 3H, CH_3). MS: *m/z* 251 (M^+). Anal. $C_{15}H_{13}N_3O$ (C, H, N).

Cell-based Assays

Compounds

Compounds were dissolved in DMSO at 100 mM and then diluted in culture medium.

Cells and Viruses

Cell lines were purchased from American Type Culture Collection (ATCC). The absence of mycoplasma contamination was checked periodically by the Hoechst staining method. Cell lines supporting the multiplication of RNA viruses were the following: Madin Darby Bovine Kidney (MDBK); Baby Hamster Kidney (BHK-21); $CD4^+$ human T-cells containing an integrated HTLV-1 genome (MT-4); Monkey kidney (Vero 76) cells.

Cytotoxicity Assays

For cytotoxicity tests, run in parallel with antiviral assays, MDBK, BHK and Vero 76 cells were resuspended in 96 multiwell plates at an initial density of $6x10^5$, $1x10^6$ and $5x10^5$ cells/mL, respectively, in maintenance medium, without or with serial dilutions of test compounds. Cell viability was determined after 48-120 hrs at 37°C in a humidified CO_2 (5%) atmosphere by the MTT method. The cell number of Vero 76 monolayers was determined by staining with the crystal violet dye.

For cytotoxicity evaluations, exponentially growing cells derived from human haematological tumors [$CD4^+$ human T-cells containing an integrated HTLV-1 genome (MT-4)] were seeded at an initial density of $1x10^5$ cells/ml in 96 well plates in RPMI-1640 medium supplemented with 10% fetal calf serum (FCS), 100 units/mL penicillin G and 100 μg/mL streptomycin. Cell cultures were then incubated at 37 °C in a humidified, 5% CO_2 atmosphere in the absence or presence of serial dilutions of test compounds. Cell viability was determined after 96 hrs at 37 °C by the 3-(4,5-dimethylthiazol-2-yl)-2,5-diphenyl-tetrazolium bromide (MTT) method [26].

Antiviral Assays

Activity of compounds against Human Immunodeficiency virus type-1 (HIV-1) was based on inhibition of virus-induced cytopathogenicity in MT-4 cells acutely infected with a multiplicity of infection (m.o.i.) of 0.01. Briefly, 50 μL of RPMI containing $1x10^4$ MT-4 were added to each well of flat-bottom microtitre trays containing 50 μL of RPMI, without or with serial dilutions of test compounds. Then, 20 μL of an HIV-1 suspension containing 100 $CCID_{50}$ were added. After a 4-day incubation, cell viability was determined by the MTT method.

Activity of compounds against Yellow fever virus (YFV) and Reo virus type-1 (Reo-1) was based on inhibition of virus-induced cytopathogenicity in acutely infected BHK-21 cells.

Activities against Bovine viral diarrhoea virus (BVDV), in infected MDBK cells, and against Respiratory syncytial virus (RSV), A-2 strain, in infected Vero 76 cells, were also based on inhibition of virus-induced cytopathogenicity.

BHK, MDBK and Vero 76 cells were seeded in 96-well plates at a density of $5x10^4$ and $3x10^4$ and $2.5x10^4$ cells/well, respectively, and were allowed to form confluent monolayers by incubating overnight in growth medium at 37 °C in a humidified CO_2 (5%) atmosphere. Cell monolayers were then infected with 50 μL of a proper virus dilution (in serum-free medium) to give an m.o.i = 0.01 (0.04 in the case of RSV). 1 hr later, 50 μL of MEM Earle's medium (Dulbecco's modified Eagle's medium for Vero/RSV), supplemented with inactivated foetal calf serum (FCS), 1% final concentration, without or with serial dilutions of test compounds, were added. After a 2-3 day incubation (5 days for Vero/RSV) at 37 °C, cell viability was determined by the MTT method. In the case of Vero/RSV, cell viability was determined with crystal violet staining of the monolayer (see below), followed by OD determination in spectrophotometer at 570 nm of the dye recovered from the monolayer solubilized with a solution containing 1% sarkosyl and Hepes 10%.

Activity of compounds against Coxsackie virus, B-2 strain (CVB-2), Polio virus type-1 (Polio-1), Sabin strain, was determined by plaque reduction assays in Vero 76 cell monolayers. To this end, Vero 76 cells were seeded in 24-well plates at a density of $2x10^5$ cells/well and were allowed to form confluent monolayers by incubating overnight in growth medium at 37°C in a humidified CO_2 (5%) atmosphere. Then, monolayers were infected with 250 μL of proper virus dilutions to give 50-100 PFU/well. Following removal of unadsorbed virus, 500 μL of Dulbecco's modified Eagle's medium supplemented with 1% inactivated FCS and 0.75% methyl cellulose, without or with serial dilutions of test compounds, were added. Cultures were incubated at 37 °C for 2 (Sb-1), 3 (CVB-2), days and then fixed with PBS containing 50% ethanol and 0.8% crystal violet, washed and air-dried. Plaques were then counted. 50% effective concentrations (EC_{50}) were calculated by linear regression technique.

Molecular Modeling

The 3D model structure of the Polio (Sb-1) helicase, presently not available in the Protein Data Bank (PDB), was built by a combination of homology-based techniques [27]. Briefly, the Modeller program [28-29] was employed to build a preliminary 3D model of the enzyme (reference structure PDB entry code 1SQ5, chain A [30]). The complete

3D model structure of the Polio helicase obtained with our procedure was refined by several, gradual energy minimization rounds. The Amber 7.0 software [31] with the Cornell *et al.* (*parm94*) parameter set [32] was used to this purpose. The quality of the model was assessed by using different validation tools [33-34]. Ramachandran plot statistics indicated that 94% of the main-chain dihedral angles were found in the most favourable region, thus confirming the good quality of the 3D model of the Polio helicase obtained. This optimized 3D model was then used as the entry point for molecular dynamics (MD) simulations. The putative binding site of title compounds on the Polio helicase was determined using the ActiveSite_Search option of the Binding Site module of InsightII (v. 2001, Accelrys, San Diego, USA). ActiveSite_Search identifies protein active sites or binding sites by locating cavities in the protein structure. According to the Site Search algorithm employed, the protein is first mapped onto a grid which covers the complete protein space. The grid points are then defined as free points and protein points. The protein points are grid points, within 2 Å from a hydrogen atom or 2.5 Å from a heavy atom. Then, a cubic eraser moves from the outside of the protein toward the center to remove the free points until the opening is too small for it to move forward. Those free points not reached by the eraser will be defined as site points. After a site is located, it can be modified by expanding or contracting the site. One layer of grid points at the cavity opening site will be added or removed by each expand or contract operation, respectively.

The model structures of title compounds were generated using the Biopolymer module of Insight II. All molecules were subjected to an initial energy minimization, again using the *sander* module of the Amber 7.0 suite of programs, with the *parm94* version of the Ambere field. The convergence criterion was set to 10^{-4} kcal/(mol Å). A conformational search was carried out using a well-validated combined molecular mechanics/molecular dynamics simulated annealing (MDSA) protocol [35-38]. Accordingly, the relaxed structures were subjected to 5 repeated temperature cycles (from 298 K to 1000 K and back) using constant volume/constant temperature (NVT) MD conditions. At the end of each annealing cycle, the structures were again energy minimized to converge below 10^{-4} kcal/(mol Å), and only the structures corresponding to the minimum energy were used for further modelling. The atomic partial charges for the geometrically optimized compounds were obtained using the RESP procedure [39], and the electrostatic potentials were produced by single-point quantum mechanical calculations at the Hartree-Fock level with a 6-31G* basis set, using the Merz-Singh-Kollman van der Waals parameters [40].

The optimized structures of all compounds were docked into the putative Polio helicase binding site following to a validated procedure [36,38,41]; accordingly, it will be described here only briefly. The software AutoDock 3.0 [42] was employed to estimate the possible binding orientations of all compounds in the receptor. In order to encase a reasonable region of the protein surface and interior volume, centered on the identified binding site, the grids were 40 Å on each side. Grid spacing (0.375 Å), and 80 grid points were applied in each Cartesian direction so as to calculate mass-centered grid maps. Amber 12-6 and 12-10 Lennard-Jones parameters were used in modelling van der Waals interactions and hydrogen bonding (N-H, O-H and S-H), respectively. In the generation of the electrostatic grid maps, the distance dependent relative permittivity of Mehler and Solmajer [43] was applied.

For the docking of each compound to the protein, three hundred Monte Carlo/Simulated Annealing (MC/SA) runs were performed, with 100 constant temperature cycles for simulated annealing. For these calculations, the GB/SA implicit water model [44] was used to mimic the solvated environment. The rotation of the angles ϕ and φ, and the angles of side chains were set free during the calculations. All other parameters of the MC/SA algorithm were kept as default. Following the docking procedure, all structures of compounds were subjected to cluster analysis with a tolerance of 1 Å for an all-atom root-mean-square (RMS) deviation from a lower-energy structure representing each cluster family. In the absence of any relevant crystallographic information, the structure of each resulting complex characterized by the lowest interaction energy was selected for further evaluation.

Each best substrate/helicase complex resulting from the automated docking procedure was further refined in the Amber suite using the quenched molecular dynamics method (QMD) [45]. In this case, 100 ps MD simulation at 298 K were employed to sample the conformational space of the substrate-enzyme complex in the GB/SA continuum solvation environment [44]. The integration step was equal to 1 fs. After each ps, the system was cooled to 0 K, the structure was extensively minimized, and stored. To prevent global conformational changes of the enzyme, the backbone of the protein binding site were constrained by a harmonic force constant of 100 kcal/Å, whereas the amino acid side chains and the ligands were allowed moving without any constraint.

The best energy configuration of each complex resulting from the previous step was solvated by adding a sphere of TIP3P water molecules [46] with a 30 Å radius from the mass center of the ligand with the use of the cap option of the *leap* module of Amber 7.0. The protein-complex was neutralized adding a suitable number of counterions (Na^+ and Cl^-) in the positions of largest electrostatic potential, as determined by the module *cion* of the Amber platform. The counterions, which had distances larger than 25 Å from the active site, were fixed in space during all simulations to avoid artifactual long range electrostatic effects on the calculated free energies. After energy minimization of the water molecules for 1500 steps, and MD equilibration of the water sphere with fixed solute for 20 ps, further unfavourable interactions within the structures were relieved by progressively smaller positional restraints on the solute (from 25 to 0 kcal/(mol $Å^2$) for a total of 4000 steps. Each system was gradually heated to 298 K in three intervals, allowing a 5 ps interval per each 100 K, and then equilibrated for 50 ps at 298 K, followed by 400 ps of data collection runs, necessary for the estimation of the free energy of binding (*vide infra*).

After the first 20 ps of MD equilibration, additional TIP3P water molecules were added to the 30 Å water cap to compensate for those who were able to diffuse into gaps of the enzyme. The MD simulations were performed at 298 K using the Berendsen coupling algorithm [47], an integration time step of 2 fs, and the applications of the *shake* algorithm [48] to constrain all bonds to their equilibrium values, thus removing high frequency vibrations. Long-range nonbonded interactions were truncated by using a 30 Å residue-based cut-off. For the calculation of the binding free energy between Polio helicase and title compounds in water, a total of 400 snapshots were saved during the MD data collection period described above, one snapshot per each 1 ps of MD simulation. The binding free energy ΔG_{bind} of each complex in water was calculated according to the procedure termed MM/PBSA (Molecular Mechanic/Poisson-Boltzmann Surface Area) and proposed by Srinivasan *et al.* [49]. Since the theoretical background of this methodology is described in details in the original paper, it will be only briefly described below. Following the MM/PBSA theory, the binding free energy between a given title compound and the target enzyme can be calculated as:

$$\Delta G_{bind} = \Delta E_{MM} + \Delta G_{solv} - T\Delta S \quad (1)$$

where:

$$\Delta G_{solv} = \Delta G_{PB} + \Delta G_{NP} \quad (2)$$

ΔE_{MM} denotes the sum of molecular mechanics (MM) energies of the molecules, and can be further split into contributions from electrostatic (ΔE_{EL}) and van der Waals (ΔE_{vdW}) energies:

$$\Delta E_{MM} = \Delta E_{EL} + \Delta E_{vdW} \quad (3)$$

The terms in equation (3) were calculated by using the *carnal* and *anal* modules of AMBER 7. ΔG_{solv} represents the solvation free energy. The polar solvation process (i.e., ΔG_{PB} in eq. (2)) is equivalent to the transfer of a protein from one medium with dielectric constant equal to that of the interior of the protein to another medium with dielectric constant equal to that of the exterior of the protein. This term yields a free energy because it corresponds to the work done to reversibly charge the solute, and it is a polarization free energy because the work goes to the polarization of the solvent. The non polar solvation contribution (i.e., ΔG_{NP} in eq. (2)) includes cavity creation in water and van der Waals interactions between the modelled nonpolar protein and water molecules. This term can be imagined as transferring a nonpolar molecule with the shape of the protein from vacuum to water. The polar component of ΔG_{solv} was evaluated with the Poisson-Boltzmann (PB) approach [50]. This procedure involves using a continuum solvent model, which represents the solute as a low dielectric medium (i.e. of dielectric constant $\varepsilon = 1$) with embedded charges and the solvent as a high dielectric medium ($\varepsilon = 80$) with no salt. All atomic charges were taken from the Cornell *et al.* force field and from our *ab initio* calculations (see above), since these are consistent with the MM energy calculations. The dielectric boundary is the contact surface between the radii of the solute and the radius (1.4 Å) of a water molecule. The numerical solution of the linearized Poisson-Boltzmann equations were solved on a cubic lattice by using the iterative finite-difference method implemented in the DelPhi software package [51]. The grid size used was 0.5 Å. Potentials at the boundaries of the finite-difference lattice were set to the sum of the Debye-Hückel potentials. The non-polar contribution to the solvation energy was calculated as $\Delta G_{NP} = \gamma$ (SASA) + β, in which $\gamma = 0.00542$ kcal/Å^2, $\beta = 0.92$ kcal/mol, and SASA is the solvent-accessible surface estimated with the MSMS program [52].

The normal-mode analysis approach was followed to estimate the last parameter, i.e. the change in solute entropy upon association $-T\Delta S$ [53]. In the first step of this calculation, an 8-Å sphere around each title compound was cut out from an MD snapshot for each inhibitor-protein complex. This value was shown to be large enough to yield converged mean changes in solute entropy. On the basis of the size-reduced snapshots of the complex, we generated structures of the uncomplexed reactants by removing the atoms of the protein and ligand, respectively. Each of those structures was minimized, using a distance-dependent dielectric constant $\varepsilon = 4r$, to account for solvent screening, and its entropy was calculated using classical statistical formulas and normal mode-analysis. To minimize the effects due to different conformations adopted by individual snapshots we averaged the estimation of entropy over 10 snapshots.

REFERENCES

[1] Sparatore, F.; Pagani, F. *Farmaco, Ed. Sci.*, **1962**, *17*, 414.
[2] Sparatore, F.; Pagani, F. *Farmaco, Ed. Sci.*, **1965**, *20*, 248.
[3] Sparatore, F.; La Rotonda, M.I.; Paglietti, G.; Ramundo, E.; Silipo, C.; Vittoria, A. *Farmaco, Ed. Sci.*, **1978**, *33*, 901.
[4] Sparatore, F.; Pagani, F.; Caliendo, G.; Novellino, E.; Silipo, C.; Vittoria, A. *Farmaco, Ed. Sci.*, **1988**, *43*, 141.
[5] Boido, A.; Vazzana, I.; Sparatore, F.; Cappello, B.; Diurno, V.; Matera, C.; Marrazzo, R.; Russo, S.; Cenicola, M.L.; Marmo, F. *Farmaco*, **1989**, *44*, 257.
[6] Loriga, M.; Paglietti, G.; Sparatore, F.; Pinna, G.; Sisini, A. *Farmaco*, **1992**, *47*, 439.
[7] Paglietti, G.; Sanna, P.; Carta, A.; Sparatore, F.; Vazzana, I.; Peana, A.; Satta, M. *Farmaco*, **1994**, *49*, 693.
[8] Vazzana, I.; Boido, A.; Sparatore, F.; Di Carlo, R.; Mattace Raso, G.; Pacilio, M. *Farmaco*, **1997**, *52*, 131.
[9] Paglietti, G.; Sparatore, F. *Farmaco, Ed. Sci.*, **1972**, *27*, 380.
[10] Paglietti, G.; Sparatore, F. *Ann. Chim.*, **1972**, *62*, 128.
[11] Carta, A.; Sanna, P.; Paglietti, G.; Sparatore, F. *Heterocycles*, **2001**, *55*, 1133.
[12] Sanna, P.; Carta, A.; Paglietti, G.; Zanetti, S.; Fadda, G. *Farmaco*, **1992**, *47*, 1001.
[13] Sanna, P.; Carta, A.; Paglietti, G.; Bacchi, A.; Pelizzi, G. *J. Heterocyclic Chem.*, **1997**, *34*, 97.
[14] Carta, A.; Sanna, P.; Molinari, H. *Heterocycles*, **1997**, *45*, 1391.
[15] Sanna, P.; Carta, A.; Paglietti, G. *Heterocycles*, **1999**, *51*, 2171.
[16] Carta, A.; Sanna, P.; Bacchi, A. *Heterocycles*, **2002**, *57*, 1079.
[17] Sanna, P.; Carta, A.; Rahbar Nikookar, M.E. *Eur. J. Med. Chem.*, **2000**, *35*, 535.
[18] Sanna, P.; Carta, A.; Gherardini, L.; Rahbar Nikookar, M.E. *Farmaco*, **2002**, *57*, 79.
[19] Carta, A.; Sanna, P.; Palomba, M.; Vargiu, L.; La Colla, M.; Loddo, R. *Eur. J. Med. Chem.*, **2002**, *37*, 891.
[20] Carta, A.; Palomba, M.; Boatto, G.; Busonera, B.; Mureddu, M.; Loddo, R. *Farmaco*, **2004**, *59*, 637.
[21] Ochoa, C.; Rodriguez, J. *J. Heterocyclic Chem.*, **1997**, *34*, 1053.

[22] Charlton, P.T.; Maliphant, G.K.; Oxley, P.; Peak, D.A. *J. Chem. Soc.*, **1951**, 485.
[23] Yu, K.; Civiello, R.L.; Combrink, K.D.; Gulgeze, H.B.; Sin, N.; Wang, X.; Meanwell, N.A.; Venables, B.L. Imidazopyridine and imidazopyrimidine antiviral agents, **2002** US patent 6,489,338 B2.
[24] Yu, K.; Civiello, R.L.; Combrink, K.D.; Gulgeze, H.B.; Sin, N.; Pearce, B.C.; Wang, X.; Meanwell, N.A.; Zhang, Y. Benzimidazolone antiviral agents, **2003** US patent 6,506,738 B1.
[25] Lackey, J.W.; Kinder, D.S.; Tuermoes, N.A. Benzimidazole compounds and antiviral uses thereof, **2003** US patent 0119754 A1.
[26] Pauwels, R.; Balzarini, J.; Baba, M.; Snoeck, R.; Schols, D.; Herdewijn, P.; Desmyster, J.; De Clercq, E. *J. Virol. Methods.*, **1998**, *20*, 309.
[27] Marti-Renom, M.A.; Stuart, A.; Fiser, A.; Sánchez, R.; Melo, F.; Sali, A. *Annu. Rev. Biophys. Biomol. Struct.*, **2000**, *29*, 291.
[28] Sali, A.; Blundell, TL. *J. Mol Biol.*, **1993**, *234*, 779.
[29] Sali, A.; Potterton, L.; Yuan, F.; van Vlijmen, H.; Karplus, M. *Proteins*, **1995**, *23*, 318.
[30] Ivey, R.A.; Zhang, Y.M.; Virga, K.G.; Hevener, K.; Lee, R.E.; Rock, C.O.; Jackowski, S.; Park, H.W.; *J. Biol. Chem.*, **2004**, *279*, 35622.
[31] Case, D.A.; Pearlman, D.A.; Caldwell, J.D.; Cheatham III, T.E.; Wang, J.; Ross, W.S.; Simmerling, C.; Darden, T.A.; Merz, K.M.; Stanton, R.V.; Cheng, A.L.; Vincent, J.J.; Crowley, M.; Tsui, V.; Gohlke, H.; Radmer, R.J.; Duan, Y.; Pitera, J.; Massova, I.; Seibel, G.L.; Singh, U.C.; Weiner, P.K.; Kollman, P.A.; **2002**, AMBER 7 University of California, San Francisco, CA, USA.
[32] Cornell, W.D.; Cieplak, P.; Bayley, C.I.; Gould, I.; Merz, K.M.; Ferguson, D.M.; Spellmeyer, D.C.; Fox, T.; Caldwell, J.W.; Kollman, P.A. *J. Am. Chem. Soc.*, **1995**, *117*, 5179.
[33] Laskowski, R.A.; MacArthur, M.W.; Moss, D.S.; Thornton, J.M.; *J. Appl. Crys.*, **1993**, *26*, 283.
[34] Rhodriguez, R.; Chinea, G.; Lopez, N.; Pons, T.; Vriend, G. *CABIOS*, **1998**, *14*, 523.
[35] Fermeglia, M.; Ferrone, M.; Pricl, S. *Bioorg. Med. Chem.*, **2002**, *10*, 2471.
[36] Felluga, F.; Pitacco, G.; Valentin, E.; Coslanich, A.; Fermeglia, M.; Ferrone, M.; Pricl, S. *Tetrahedron Asymmetry*, **2003**, *14*, 3385.
[37] Manfredini, S.; Solaroli, N.; Angusti, A.; Nalin, F.; Durini, E.; Vertuani, S.; Pricl, S.; Ferrone, M.; Spadari, S.; Focher, F.; Verri, A.; De Clercq, E.; Balzarini, J. *J. Antivir. Chem. Chemother.*, **2003**, *14*, 183.
[38] Mamolo, M.G.; Zampieri, D.; Vio, L.; Fermeglia, M.; Ferrone, M.; Pricl, S.; Scialino, G.; Banfi, E. *Bioorg. Med. Chem.*, **2005**, *13*, 3797.
[39] Bayly, C.I.; Cieplak, P.; Cornell, W.D.; Kollman, P.A. *J. Phys. Chem.*, **1993**, *97*, 10269.
[40] Besler, B.H.; Merz, K.M.; Kollman, P.A. *J. Comput. Chem.*, **1990**, *11*, 431.
[41] Felluga, F.; Fermeglia, M.; Ferrone, M.; Pitacco, G.; Pricl, S.; Valentin, E. *Tetrahedron Asymmetry*, **2002**, *13*, 475.
[42] Morris, G.M.; Goodsell, D.S.; Halliday, R.S.; Huey, . R.; Hart, W.E.; Belew, R.K.; Olson, A.J. *J. Comput. Chem.*, **1998**, *19*, 1639.
[43] Mehler, E.L., Solmajer, T. *Protein Eng.*, **1991**, *4*, 903.
[44] Jayaram, B.; Sprous, D.; Beveridge, D.L.; *J. Phys. Chem. B*, **1998**, *102*, 9571.
[45] Frecer, V.; Kabelac, M.; De Nardi, P.; Pricl, S.; Miertus, S. *J. Mol. Graph. Model.*, **2004**, *22*, 209.
[46] Jorgensen, W.L.; Chandrasekhar, J.; Madura, J.D.; Impey, R.W.; Klein, M.L. *J. Comput. Phys.*, **1983**, *79*, 926.
[47] Berendsen, H.J.C.; Postma, J.P.M.; van Gunsteren, W.F.; DiNola, A.; Haak, J.R. *J. Comput. Phys.*, **1984**, *81*, 3684.
[48] Ryckaert, J.P.; Ciccotti, G.; Berendsen, H.J.C. *Comput. Phys.*, **1977**, *23*, 327.
[49] Srinivasan, J.; Cheatham III, T.E.; Cieplak, P.; Kollman, P.A.; Case, D.A. *J. Am. Chem. Soc.*, **1998**, *120*, 9401.
[50] Gilson, M.K.; Sharp, K.A.; Honig, B.H. *J. Comput. Chem.*, **1987**, *9*, 327.
[51] Sitkoff, D.; Sharp, K.A.; Honig, B.H. *J. Phys. Chem.*, **1994**, *98*, 1978.
[52] Sanner, M.F.; Olson, A.J.; Spehner, J.C. *Biopolymers*, **1996**, *38*, 305.
[53] Wilson, E.B.; Decius, J.C.; Cross, P.C. *Molecular Vibrations*; McGraw-Hill: New York, **1955**.

Received: 31 March, 2006 **Revised: 28 April, 2006** **Accepted: 29 April, 2006**

Volume 6, Number 11, November 2006

ISSN: 1389-5575

Mini Reviews in ... Medicinal Chemistry

The international journal for timely mini reviews in Medicinal Chemistry

BENTHAM SCIENCE PUBLISHERS LTD.